Available online at www.sciencedirect.com
SCIENCE DIRECT®
Biochemical and Biophysical Research Communications 319 (2004) 83–94
BBRC
www.elsevier.com/locate/ybbrc

Rab11-FIP3 localises to a Rab11-positive pericentrosomal compartment during interphase and to the cleavage furrow during cytokinesis

Conor P. Horgan, Melanie Walsh,[1] Tomas H. Zurawski,[1] and Mary W. McCaffrey*

Molecular Cell Biology Laboratory, Department of Biochemistry, Biosciences Institute, University College Cork, Cork, Ireland

Received 15 March 2004

Abstract

The Rab11-family interacting protein 3 (Rab11-FIP3), also known as Arfophilin and Eferin, is a Rab11 and ADP-ribosylation factor (ARF) binding protein of unknown function. Here, we sought to investigate the subcellular localisation and elucidate the function of Rab11-FIP3 in eukaryotic membrane trafficking. Utilising a polyclonal antibody specific for Rab11-FIP3, we have demonstrated by immunofluorescence microscopy that Rab11-FIP3 colocalises with Rab11 in a distinctive pericentrosomal location in A431 cells. Additionally, we found that Rab11-FIP3 localises to punctate vesicular structures dispersed throughout A431 cells. We have demonstrated that both Rab11 and Rab11-FIP3 localise to the cleavage furrow during cytokinesis, and that Rab11-FIP3 localisation is dependent on both microtubule and actin filament integrity. We show that Rab11-FIP3 does not enter brefeldin A (BFA) induced membrane tubules that are positive for the transferrin receptor (TfnR). Furthermore, we show that expression of an amino-terminally truncated mutant of Rab11-FIP3 (Rab11-FIP3$_{(244–756)}$) does not inhibit transferrin (Tfn) recycling in HeLa cells. It is likely that Rab11-FIP3 is involved in trafficking events other than Tfn trafficking; these may include the transport of endosomally derived membrane to the cleavage furrow during cytokinesis.

Keywords: Rab11-FIP3; Arfophilin; Rab11; ADP-ribosylation factor; Rab11-FIP4; RCP; Rab11-FIP2; Endosomal recycling compartment; Cleavage furrow; Cytokinesis; Nuf

In order to maintain cellular homeostasis, eukaryotic cells are required to tightly regulate the transport of lipids and proteins within the cell. Intracellular transport typically occurs via vesicles that bud from a donor compartment, navigate through the cytoplasm, and then dock and fuse with an acceptor compartment. In this context, the ARF and Rab families of low molecular weight GTPases have emerged as central regulators of the various membrane trafficking events [3,21,41].

To date, six mammalian ARF genes have been cloned. They have been categorised into three classes based on their primary structure: class I (ARF1, 2, and 3), class II (ARF4 and 5), and class III (ARF6). Class I ARFs control the formation of several different types of coated vesicles and are involved in trafficking in the endoplasmic reticulum (ER), Golgi, and endosomal systems [2,7,8]. Data on the roles of class II ARFs are limited, but they appear to play similar roles to those of class I ARFs [2,13,17]. The class III ARF, ARF6, functions in endosomal recycling to the plasma membrane, regulation of secretion, and coordinating actin cytoskeleton changes at the plasma membrane [3,5]. More recently, it has been shown that ARF6 is implicated in cleavage furrow ingression and cytokinesis since both its localisation and its activated (GTP-bound) levels change during mitotic progression [30].

Each Rab GTPase is thought to regulate the budding, trafficking, and/or docking of transport vesicles along discrete transport steps [41]. Rab4 and Rab11 are implicated in the endosomal recycling processes. Rab4 has been localised to the early endosomes, and studies on Tfn recycling in cells expressing mutant forms of Rab4

* Corresponding author. Fax: +353-21-4901379.
E-mail address: m.mccaffrey@ucc.ie (M.W. McCaffrey).
[1] These authors contributed equally to this work.

0006-291X/$ - see front matter © 2004 Elsevier Inc. All rights reserved.
doi:10.1016/j.bbrc.2004.04.157

have implicated it in the regulation of membrane receptor recycling and trafficking to late endosomes [36,37]. On the other hand, Rab11 localises predominantly to the endosomal recycling compartment (ERC), and has been shown to function in endocytic recycling from the ERC to the plasma membrane [35]. Rab11 is also found associated with the *trans*-Golgi network (TGN), and has been reported to regulate trafficking between the ERC and the TGN [40]. Furthermore, while several studies have now implicated Rab11 in cytokinesis [4,6,26,34], the molecular details of such a role remain unclear.

During the past few years, much attention by various groups has been focused on the identification of novel ARF and Rab11 effectors. This resulted in the identification of Arfophilin, a class II ARF effector [32], that was later shown to also interact with the class III ARF, ARF6 [31,32]. Subsequent to this, in searches for Rab11 effectors Arfophilin was rediscovered as Rab11-FIP3 [9] and as Eferin [25]. Due to the nomenclature complexity, Rab11-FIP3/Arfophilin/Eferin will henceforth be referred to as Rab11-FIP3.

Rab11-FIP3 was initially reported as a cDNA clone (KIAA0665) isolated from human brain [23]. It has been shown to bind class II and class III ARFs as well as all the Rab11 subfamily members (Rab11a, Rab11b, and Rab25) in a GTP dependent manner [9,31,32], and to colocalise with Rab11a in transiently transfected HeLa cells [9]. The amino terminus of class II ARFs (amino acid residues 1–17), was shown bind the carboxy-terminal region of Rab11-FIP3 (amino acid residues 612–756) [32]. In the case of ARF6, amino acid residues 37–80 were shown to be involved in the interaction [31]. The interaction of Rab11-FIP3 with Rab11 occurs via a 20 amino acid motif, termed the Rab11 binding domain (RBD11) which is present in the Rab11-FIP3 carboxy terminus [25]. To date, little is known about the subcellular distribution of endogenous Rab11-FIP3 or its cellular function with respect to either the ARF or Rab11 families of proteins.

In this study, we describe the intracellular localisation of endogenous Rab11-FIP3 during interphase and cytokinesis. We also present data indicating that Rab11-FIP3 does not participate in Tfn trafficking. Based on these results, and given that ARF6 and Rab11 have previously been shown to be involved in cytokinesis, we suggest that Rab11-FIP3 could be involved in the delivery of endosomally derived materials to the cleavage furrow/midbody during cell division.

Materials and methods

cDNA cloning and plasmid construction. pGEX-3X/Rab11-FIP3$_{(2–246)}$ was constructed by subcloning a 0.8-kb *Bam*HI fragment, corresponding to Rab11-FIP3$_{(2–246)}$, into pGEX-3X (Amersham Biosciences). pGFP^2-C2/Rab11 was constructed by subcloning canine Rab11 from the previously described pLex-Rab11 construct [19,20], as a 0.85-kb *Eco*RI–*Pst*I fragment into pGFP^2-C2 (kind gift from R. Pepperkok). pEGFP-C1/Rab11-FIP3$_{(2–756)}$ was constructed by subcloning the 2.4-kb *Eco*RI fragment from the previously described pGADGH/Rab11-FIP3$_{(2–756)}$ construct [38], into pEGFP-C1 (BD Biosciences Clontech). pARF6/GFP^2-N3 was constructed using a forward primer *ARF6F* (5′-AAAAGAATTCCCACCATGGGGA AGGTGCTATCCAAA-3′) and a reverse primer *ARF6R* (5′-AAAA GAATTCGAGATTTGTAGTTAGAGGTTAACC-3′) to amplify human ARF6 cDNA from pARF6/AS2 (kind gift from the C. D'Souza-Schorey group). The 0.5-kb PCR fragment was then cloned into the *Eco*RI site of pGFP^2-N3 (kind gift from R. Pepperkok). pEGFP-C3/Rab11-FIP3$_{(244–756)}$ was constructed by subcloning the 1.6-kb *Sca*I–*Eco*RI fragment from pEGFP-C1/Rab11-FIP3$_{(2–756)}$ into pEGFP-C3 (BD Biosciences Clontech). pEGFP-C1/Rab11-FIP2$_{(446–511)}$ has been described previously [20]. Constructs generated by PCR were verified by double strand sequencing.

Recombinant protein purification. Glutathione *S*-transferase (GST) fused Rab11-FIP3$_{(2–246)}$ was purified as follows: XL1 *Escherichia coli* cells were transformed with pGEX-3X/Rab11-FIP3$_{(2–246)}$. Transformants were grown to an $OD_{600} = 0.6$ and induced with 0.1 mM isopropyl-β-D-thiogalactopyranoside (Qiagen) for 1 h at 30 °C. The protein was purified using glutathione–agarose (Sigma) according to the manufacturer's instructions.

Antibodies. Mouse monoclonal anti-TfnR was purchased from Zymed Laboratories. Mouse monoclonal anti-EEA1 was obtained from Transduction Laboratories. Both mouse monoclonal anti-γ and anti-α-tubulin were purchased from Sigma and sheep polyclonal anti-TGN46 was purchased from Serotec. Mouse monoclonal (6C4) anti-lysophosphatidic acid (LBPA) was a kind gift from J. Gruenberg. The affinity-purified rabbit polyclonal anti-Rab coupling protein (RCP) antibody has been described elsewhere [19]. The affinity-purified rabbit polyclonal anti-Rab11 was prepared in the same way as anti-Rab11 described by Wilcke et al. [40]. Texas red conjugated phalloidin, which was used to visualise F-actin, was purchased from Molecular Probes.

Anti-Rab11-FIP3 antibody. Rabbit polyclonal anti-Rab11-FIP3 was generated as follows: a synthetic peptide corresponding to amino acid residues 80–97 (GGPRDPGPSAPPPRSGPR) of Rab11-FIP3 was conjugated to keyhole limpet haemocyanin (KLH) via the amino-terminal end of the peptide. This was injected into rabbits for antibody generation, following which the resulting crude IgG was affinity-purified (Davids Biotechnologie, Regensburg, Germany). The affinity-purified rabbit antiserum was used at a dilution of 1/150 for immunofluorescence, and 1/200 for immunoblotting.

Affinity-purified antibody was pre-adsorbed with 30 μg/ml purified recombinant GST tagged Rab11-FIP3$_{(2–246)}$ or with 10 μg/ml of the immunising peptide at room temperature for 2 h to block antibody binding.

Cell lines and transfection. A431 (epidermal carcinoma) and HeLa (cervical carcinoma) human cell lines were maintained in Dulbecco's modified Eagle's medium supplemented with 10% foetal bovine serum, 2 mM L-glutamine, and 100 U/ml penicillin–streptomycin and grown in 5% CO_2 at 37 °C. For overexpression studies, cells were transfected with plasmid constructs using Effectene (Qiagen) as a transfection reagent according to the manufacturer's instructions. Sixteen to eighteen hours post-transfection the cells were processed for immunofluorescence microscopy as described below.

Immunofluorescence microscopy. Cells were grown on 11 mm round glass coverslips and fixed with either methanol (for γ-tubulin staining) or 3% paraformaldehyde (PFA). The PFA fixed samples were treated as follows: free aldehyde groups were quenched with 50 mM NH_4Cl, the cells were then permeabilised with 0.05% (w/v) saponin followed by incubation with the primary antibodies diluted in 5% (v/v) foetal bovine serum/phosphate buffered saline (PBS) containing 0.05% (w/v) saponin. The secondary antibodies used were donkey anti-mouse conjugated to Texas red, donkey anti-mouse conjugated to fluorescein

isothiocyanate (FITC), donkey anti-rabbit conjugated to indocarbocyanine (Cy3), donkey anti-rabbit conjugated to cyanine (Cy2), and donkey anti-sheep conjugated to FITC (all from Jackson ImmunoResearch). Coverslips were mounted in MOWIOL (CalBiochem) which contained 100 mg/ml DABCO (Sigma) and images were recorded using a Zeiss LSM 510 META confocal microscope fitted with a 63×/1.4 plan apochromat lens. Images were processed using the Zeiss LSM Image Browser (CarlZeiss) and Adobe Illustrator (Adobe) software.

Drug treatment. Nocodazole and cytochalasin D (both from Sigma) were solubilised in dimethyl sulphoxide (DMSO). BFA (Sigma) was solubilised in methanol. A431 cells growing on glass coverslips were incubated either with 10 μM nocodazole or 10 μM cytochalasin D for 30 min at 37 °C or with 20 μg/ml BFA for 15 min at 37 °C prior to fixation and immunostaining. As a control, cells were treated with 0.2% (v/v) DMSO or 1% (v/v) methanol alone.

Alexa 594-Tfn recycling assay. The recycling experiments were performed as previously described [18]. Briefly, 16 h post-transfection (with either pEGFP-C3/Rab11-FIP3$_{(244–756)}$ or pEGFP-C1/Rab11-FIP2$_{(446–511)}$), serum starved cells were allowed to internalise Alexa 594-coupled iron saturated holotransferrin (Molecular Probes) at 5 μg/ml for 45 min at 37 °C. Cells were then briefly washed with ice-cold PBS and immediately fixed with 3% PFA. For the recycling assay, internalised Tfn was allowed to recycle by continued incubation of cells for an additional 30 min at 37 °C in the presence of 100-fold excess unlabelled holotransferrin and 0.1 mM desferroxamine (Sigma). Following recycling, cells were again washed with ice-cold PBS and immediately fixed with 3% PFA.

Immunoblotting analysis. A431 and HeLa cells were resuspended in 50 mM Tris–HCl (pH 7.4), 150 mM NaCl, 1 mM EDTA, 0.5% NP-40 plus protease inhibitors and lysed under rotation for 30 min at 4 °C. Ruptured cells were then quickly passed six times through a 26-gauge needle and centrifuged at 10,000*g* for 5 min at 4 °C. For detection of endogenous Rab11-FIP3, 200 μg of the 10,000*g* supernatant was analysed by SDS–PAGE and immunoblotting. Twenty-five micrograms of the 10,000*g* supernatant from HeLa cells transiently transfected with *pEGFP-C1/Rab11-FIP3* was used as a positive control for immunoblotting. β-Actin was used as a loading control.

Results

Polyclonal anti-Rab11-FIP3 antibody recognises endogenous Rab11-FIP3 in A431 and HeLa cells

Previous studies on Rab11-FIP3 and its biological significance have relied on the overexpression of protein. However, it is becoming increasingly apparent that the overexpression of the Rab11-FIPs causes a perturbation of the ERC morphology [11,39]. Consequently, we sought to study endogenous Rab11-FIP3 through the generation of an antibody that specifically recognises this Rab11-FIP family member. To obtain a Rab11-FIP3 specific antibody, we chose an immunising peptide that represented amino acid residues 80–97 of Rab11-FIP3. This region was chosen due to its predicted immunogenic properties and its exclusiveness to Rab11-FIP3 among the currently known Rab11-FIPs (Fig. 1A). Furthermore, the selected peptide is not conserved among any other known proteins upon BLAST analysis.

To test the ability of our antibody to recognise endogenous Rab11-FIP3, we performed Western blot analysis on A431 and HeLa cell extracts. We found that the affinity-purified antibody identified a 130-kDa band representing endogenous Rab11-FIP3 (Fig. 1B, top panel). No bands were detected by the preimmune serum (data not shown). Anti-Rab11-FIP3 also recognised a 160-kDa band that represented EGFP tagged Rab11-FIP3 (pEGFP-C1/Rab11-FIP3$_{(2–756)}$) that was exogenously expressed in HeLa cells (Fig. 1B, top panel). Furthermore, this antibody recognised 20 ng of purified recombinant Rab11-FIP3$_{(2–246)}$ but did not recognise the

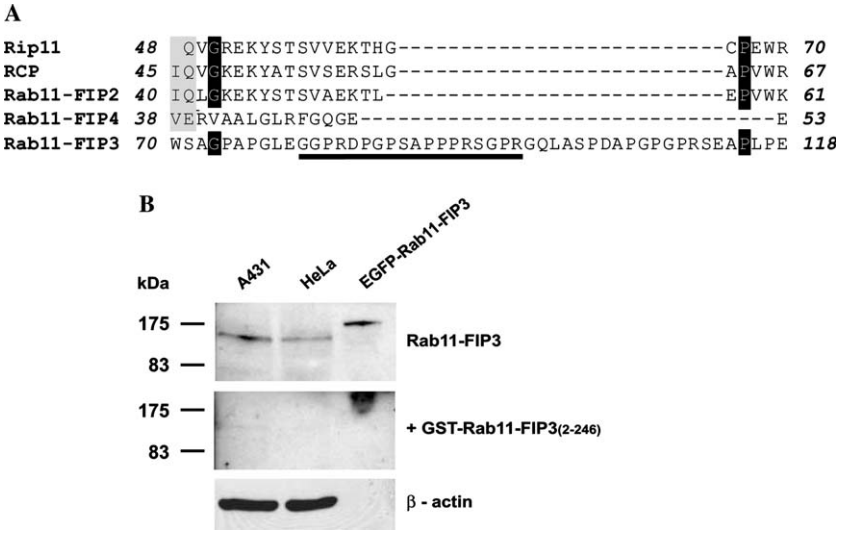

Fig. 1. Rabbit polyclonal anti-Rab11-FIP3 antibody recognises endogenous Rab11-FIP3. (A) A portion of a ClustalW alignment of the full-length amino acid sequences of the Rab11-FIP family members, which encompasses the specific immunising peptide Rab11-FIP3$_{(80–97)}$ (underlined), is shown. Identities are in black, similarities in grey. (B) Two hundred micrograms of the 10,000*g* supernatant of *A431* and *HeLa* cell lysates, and 25 μg of the 10,000*g* supernatant from HeLa cells expressing EGFP tagged Rab11-FIP3 (*EGFP-Rab11-FIP3*), were analysed by SDS–PAGE and immunoblotting with affinity-purified anti-Rab11-FIP3 antibody. Identical samples were probed with the affinity-purified antibody that had been pre-adsorbed with GST-Rab11-FIP3$_{(2–246)}$. β-Actin was monitored as a loading control. The results are representative of at least three separate experiments.

same amount of purified recombinant Rab11-FIP2, Rab11-FIP4$_{(82–637)}$, Rip11 or RCP (data not shown). Prior incubation of the affinity-purified antibody with 30 μg/ml of recombinant GST-Rab11-FIP3$_{(2–246)}$ for 2 h completely blocked antibody binding (Fig. 1B, middle panel). Identical results were obtained when the antibody was pre-incubated with 10 μg/ml of the immunising peptide for 2 h (data not shown). The blot was probed for β-actin to monitor levels of loading of the A431 and HeLa cell extracts (Fig. 1B, bottom panel). Actin was not observed in the *EGFP-Rab11-FIP3* lane, as there was eightfold less cell extract loaded in this lane relative to the other lanes. To further confirm the specificity of our Rab11-FIP3 antibody, we investigated if the antibody could detect exogenously expressed EGFP tagged Rab11-FIPs in vivo. Immunofluorescence analysis demonstrated that the anti-Rab11-FIP3 staining pattern was identical to that observed for EGFP tagged Rab11-FIP3 and that it did not detect other exogenously expressed Rab11-FIPs (data not shown). Taken together, these data demonstrate that our anti-Rab11-FIP3 antibody specifically recognises both exogenously and endogenously expressed Rab11-FIP3.

Rab11-FIP3 localises predominantly to a pericentrosomal location in A431 cells

In order to elucidate the biological function of Rab11-FIP3, we examined its localisation in both A431 and HeLa cells by immunofluorescence microscopy. Our results demonstrate that endogenous Rab11-FIP3 displays a distinctive staining pattern at a location near the nucleus in addition to a punctate vesicular pattern dispersed throughout A431 cells (Fig. 2C). To examine the localisation of endogenous Rab11-FIP3 with respect to Rab11, we transiently transfected cells with GFP^2 tagged Rab11 (pGFP^2-C2/Rab11). Fig. 2A illustrates that in A431 cells, endogenous Rab11-FIP3 displays significant colocalisation with exogenously expressed Rab11 in the distinctive Rab11-FIP3 positive compartment close to the nucleus. In contrast to A431 cells, the staining pattern of endogenous Rab11-FIP3 in HeLa cells displays a punctate vesicular pattern throughout the cell, which is occasionally (~3–5% of cells) concentrated near the nucleus (data not shown).

To investigate the localisation of exogenously expressed Rab11-FIP3, we transiently transfected HeLa

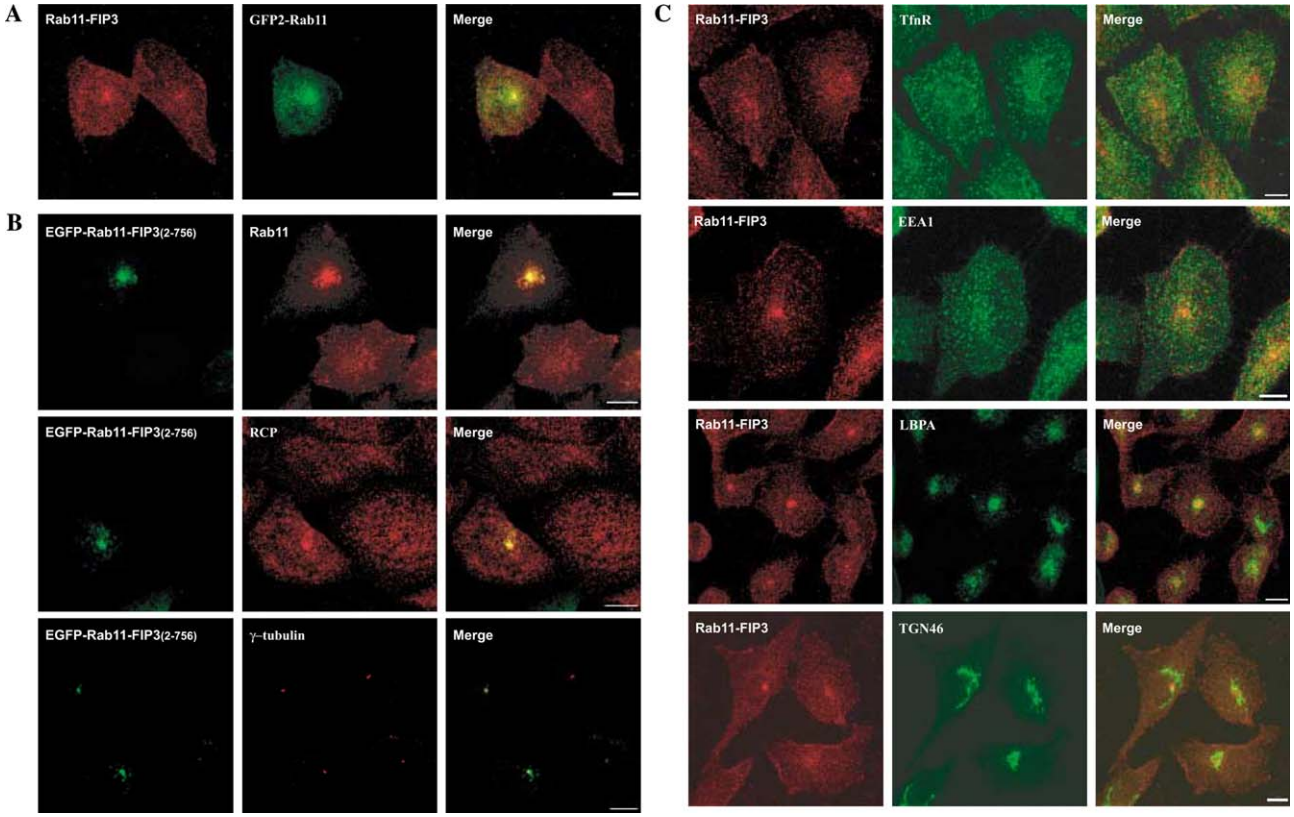

Fig. 2. Rab11-FIP3 localises predominantly to a pericentrosomal location and colocalises with Rab11. (A) A431 cells were transfected with pGFP^2-C2/Rab11. Sixteen hours post-transfection the cells were fixed in PFA, permeabilised with saponin, and immunostained with affinity-purified anti-Rab11-FIP3 antibody. (B) HeLa cells were transfected with pEGFP-C1/Rab11-FIP3$_{(2–756)}$. Sixteen to eighteen hours post-transfection the cells were processed for immunofluorescence as described in Materials and methods and immunostained with antibodies to Rab11, RCP, and γ-tubulin. (C) A431 cells were fixed and permeabilised as described in Materials and methods before immunostaining with affinity-purified anti-Rab11-FIP3 antibody and counterstaining with antibodies to TfnR, EEA1, LBPA, and TGN46. These data are typical of at least four separate experiments. Scale bar represents 10 μm.

cells with a construct encoding EGFP tagged Rab11-FIP3$_{(2–756)}$. We found that the exogenously expressed protein concentrates near the nucleus in both HeLa (*EGFP-Rab11-FIP3*$_{(2–756)}$, Fig. 2B) and A431 cells (data not shown). Immunostaining HeLa cells expressing the EGFP tagged Rab11-FIP3$_{(2–756)}$ with an anti-Rab11 antibody revealed extensive colocalisation between the exogenously expressed protein and Rab11 (Fig. 2B, top panel). Furthermore, when Rab11-FIP3 is overexpressed, it alters the Rab11 staining pattern causing it to accumulate in the Rab11-FIP3 positive compartment (compare transfected versus non-transfected cells in Fig. 2B, top panel). This contrasts with Rab11 overexpression, which does not affect the staining pattern of endogenous Rab11-FIP3 (compare Figs. 2A and B, top panel). Immunostaining HeLa cells expressing EGFP tagged Rab11-FIP3$_{(2–756)}$ with antibodies to either the TfnR or RCP revealed considerable colocalisation between these markers of the receptor recycling pathway and the exogenously expressed protein in the Rab11-FIP3 positive compartment near the nucleus (data not shown and Fig. 2B, respectively). The TfnR and RCP staining patterns normally observed in HeLa cells are perturbed upon Rab11-FIP3 overexpression. We were interested to further investigate the localisation of the distinct Rab11-FIP3 positive compartment near the nucleus. Immunostaining HeLa cells transiently expressing the protein for γ-tubulin demonstrated that this Rab11-FIP3 positive compartment surrounds the centrosome (Fig. 2B).

We next examined the localisation of endogenous Rab11-FIP3 with respect to markers of the recycling and degradative pathways and the TGN. We observed virtually no colocalisation between endogenous Rab11-FIP3 and TfnR (Fig. 2C). This finding is in contrast to what we observed when Rab11-FIP3 was exogenously expressed. However, our finding is similar to what has been previously described for Arfophilin-2/Rab11-FIP4 [11,39]. Very minor colocalisation was observed between Rab11-FIP3 and EEA1 (Fig. 2C), a Rab5 effector that localises to the early sorting endosome [22,33]. No colocalisation was observed between Rab11-FIP3 and either LBPA or TGN46 (Fig. 2C), markers of the late endosomes [15,29] and the TGN [24], respectively. Taken together, these data suggest that Rab11-FIP3 localises predominantly to a pericentrosomal Rab11 positive endosomal recycling compartment (ERC) and its overexpression alters the ERC morphology.

Rab11-FIP3 localisation is unaffected by overexpression of ARF proteins

As indicated earlier, Rab11-FIP3 is a putative class II and class III ARF effector [31,32]. Therefore, we examined the localisation of endogenous Rab11-FIP3 with respect to that of overexpressed ARF4, -5, and -6, in both A431 and HeLa cells. In interphase cells we observed no colocalisation between the respective sets of proteins, nor did we observe any effect on the localisation of endogenous Rab11-FIP3 in cells overexpressing the respective ARF proteins (data not shown). Furthermore, we sought to determine if, as reported for the closest homologue of Rab11-FIP3, Rab11-FIP4/Arfophilin-2 [11], overexpression of ARF mutants could alter the localisation of the endogenous protein. Similar to what we observed when we overexpressed the wild-type ARF proteins, no discernible effect on the localisation of the endogenous Rab11-FIP3 was evident in cells overexpressing either the GTP or GDP-locked mutants of ARF4, -5 or -6 (data not shown).

Rab11 and Rab11-FIP3 localise to the cleavage furrow during cytokinesis

In recent years a considerable amount of data has been published that implicates Rab11 in cytokinesis [4,6,26,34]. With this in mind, we used immunofluorescence microscopy to determine the localisation of Rab11 in cells undergoing cytokinesis. Upon immunostaining HeLa cells for Rab11, we found that in dividing cells, a substantial proportion of Rab11 had shifted from its perinuclear localisation (interphase) and had located to the cleavage furrow (Fig. 3A). Examination of the localisation of endogenous Rab11-FIP3 in A431 (data not shown) and HeLa cells revealed that a proportion of Rab11-FIP3 had relocated to the cleavage furrow and to the intercellular bridge during telophase/cytokinesis (Fig. 3B). Similar data were observed when Rab11-FIP3 was exogenously expressed (data not shown).

As previously mentioned, Rab11-FIP3 (Arfophilin) is a putative ARF6 effector [31]. ARF6 has been shown to become activated and to localise predominantly to the cleavage furrow during anaphase and telophase, and to the midbody during cytokinesis [30]. With this information in mind, and together with the above findings, we were prompted to investigate the localisation of Rab11-FIP3 with respect to ARF6 in cells undergoing the latter stages of cell division. In cells undergoing cytokinesis that were transiently transfected with GFP[2] tagged ARF6 and immunostained for endogenous Rab11-FIP3, we observed that ARF6 had concentrated at the midbody and that this ARF6 positive structure also displayed minor staining for Rab11-FIP3 (Fig. 3C).

Rab11-FIP3 localisation is dependent on the integrity of both the microtubule and actin cytoskeleton

It has been documented that the integrity of the ERC, as well as the localisation of other Rab11-FIP family members, is dependent on the microtubule cytoskeleton

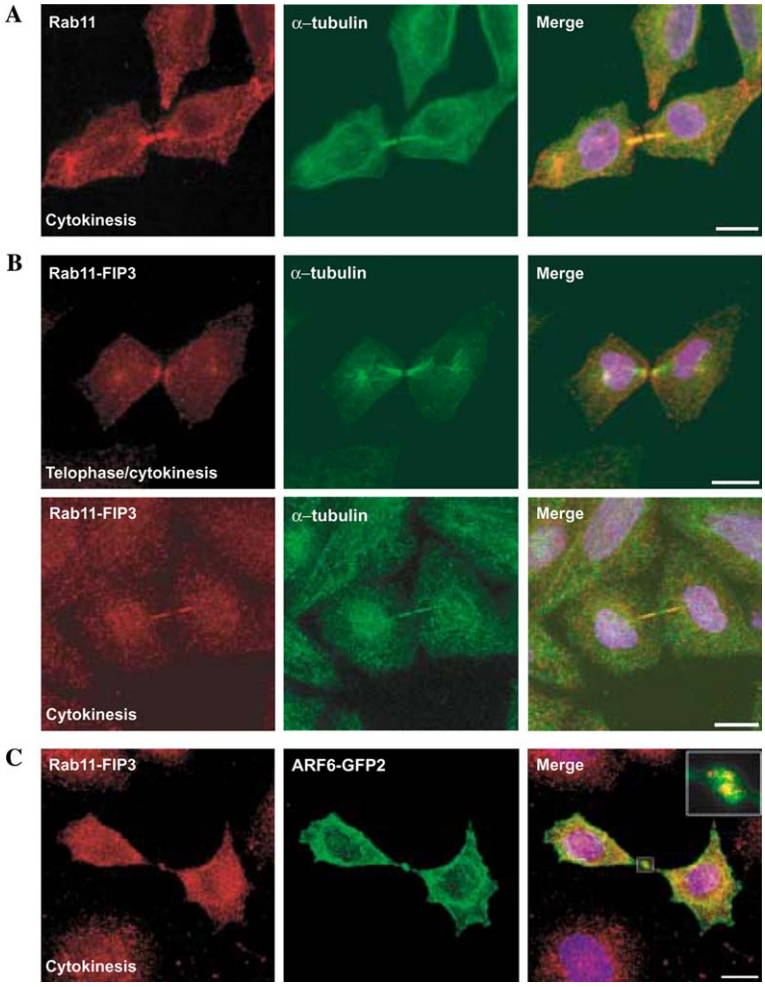

Fig. 3. Endogenous Rab11 and Rab11-FIP3 localise to the cleavage furrow during cytokinesis. HeLa cells were fixed with PFA, permeabilised with saponin, and immunostained with antibodies to either Rab11 (A), or Rab11-FIP3 (B). (C) HeLa cells were transfected with pARF6/GFP^2-N3. Sixteen hours post-transfection the cells were fixed and permeabilised as described in Materials and methods and immunostained with anti-Rab11-FIP3 antibody. Hoechst dye was used to visualise the nuclei. Scale bar represents 10 μm.

[1,11,20]. Thus, we investigated whether the cellular localisation of Rab11-FIP3 was altered by disruption of the microtubule network upon nocodazole treatment. A431 cells were treated with either 10 μM nocodazole to depolymerise the microtubules or with DMSO (drug solvent), as a control. As demonstrated in Fig. 4A, treatment of the cells with nocodazole resulted in the breakdown of the microtubule cytoskeleton. This caused the pericentrosomal Rab11-FIP3 compartment to fragment and peripherally distribute within the cell. This finding corresponds to what we observed when cells overexpressing EGFP tagged Rab11-FIP3 were treated with nocodazole (data not shown).

As Rab11-FIP3 contains a predicted ERM (erzin–radixin–moesin) domain that contains a putative binding site for actin, we investigated whether the intracellular localisation of Rab11-FIP3 is altered by disruption of the actin cytoskeleton. A431 cells were treated with either 10 μM cytochalasin D to depolymerise the actin filaments or with DMSO (drug solvent), as a control. Following depolymerisation of the actin cytoskeleton, the concentrated perinuclear localisation of Rab11-FIP3 remained unaffected (Fig. 4B). Similar data were observed when Rab11-FIP3 was exogenously expressed (data not shown). However, we found that the staining pattern of the peripherally localised endogenous Rab11-FIP3 was altered upon treatment with 10 μM cytochalasin D. Furthermore, it displayed a staining pattern coincident with that of the depolymerised actin (Fig. 4B). This suggests that the peripheral population of Rab11-FIP3 vesicles is associated with the actin cytoskeleton.

The above data demonstrate that two distinct populations of Rab11-FIP3 exist within the cell. The first at a microtubule dependent pericentrosomal location, where it colocalises with Rab11, and the second dispersed throughout the cell in association either directly or indirectly with the actin cytoskeleton.

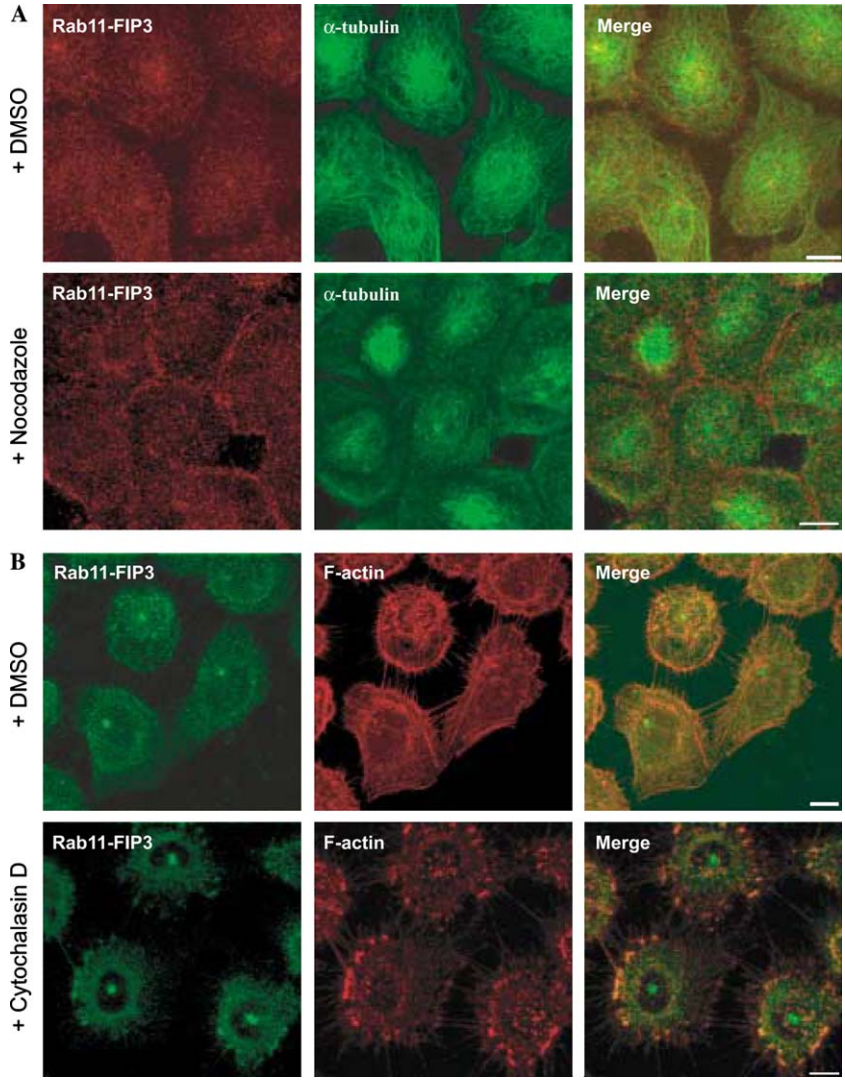

Fig. 4. Rab11-FIP3 localisation is dependent on microtubule and actin cytoskeletal integrity. A431 cells were treated with nocodazole (A) or cytochalasin D (B). In both cases DMSO was used as a control. The cells were fixed, processed for immunofluorescence analysis, immunostained with affinity-purified anti-Rab11-FIP3 antibody, and counterstained for α-tubulin (A) or F-actin (B). These experiments were repeated four times with similar results. Scale bar represents 10 μm.

BFA treatment induces tubulation of the TfnR positive network but Rab11-FIP3 localisation remains unaffected

We next studied the effects of brefeldin A (BFA) on the intracellular localisation of Rab11-FIP3. BFA is a fungal metabolite that disrupts the Golgi by inhibiting guanine nucleotide exchange factor (GEF) activity, which is required for the activity of ARF GTPases. It has been shown to disrupt intracellular membrane transport and to affect the localisation of endogenous Rab11-FIP4/Arfophilin-2 [11,14]. To determine if BFA treatment affected the localisation of Rab11-FIP3, A431 cells were treated with either 20 μg/ml BFA or with methanol (drug solvent), as a control. Treatment with methanol alone did not affect the localisation of any of the proteins (data not shown). However, treatment of cells with BFA disrupted the *trans*-Golgi network causing TGN46 to enter an elaborate tubular network (Fig. 5A). We found that this tubular network induced by BFA treatment was also strongly positive for the TfnR (Fig. 5B). Interestingly, Rab11-FIP3 does not enter these tubules and remains unaffected by BFA treatment (Figs. 5A and C).

Expression of EGFP tagged Rab11-FIP3$_{(244–756)}$ does not inhibit Tfn recycling in HeLa cells

As previously reported, the carboxy-terminal region of other Rab11-FIP family members is sufficient to confer their membrane association in vivo [19,20,39]. Furthermore, it has been demonstrated that while the expression of the carboxy-terminal regions of RCP and Rab11-FIP2 inhibits Tfn recycling [19,20], the equivalent region of Arfophilin-2/Rab11-FIP4 does not

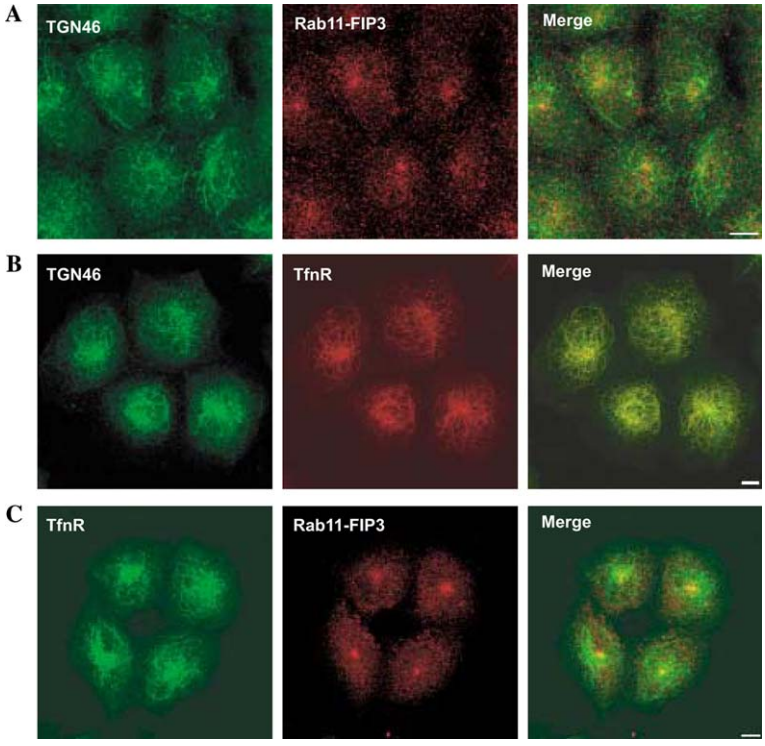

Fig. 5. BFA treatment induces tubulation of the TfnR positive network but Rab11-FIP3 localisation remains unaffected. A431 cells were treated with BFA to disrupt the Golgi. Following fixation and processing for immunofluorescence analysis, the cells were immunostained for TGN46 and Rab11-FIP3 (A), TGN46 and TfnR (B) or TfnR and Rab11-FIP3 (C). These experiments were repeated four times with similar results. Scale bar represents 10 μm.

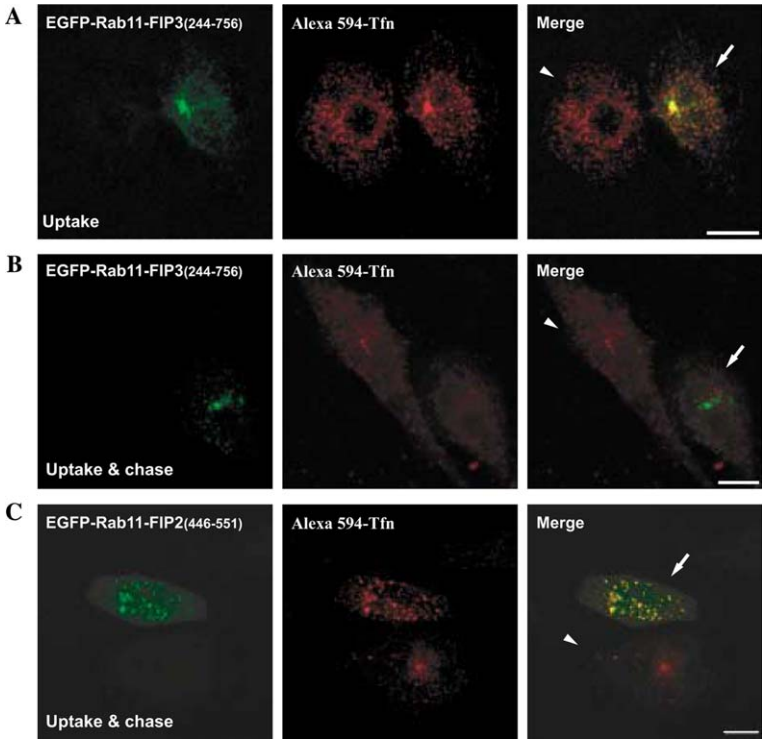

Fig. 6. Expression of an N-terminally truncated mutant of Rab11-FIP3 does not inhibit Tfn recycling. HeLa cells expressing pEGFP-C3/Rab11-FIP3$_{(244–756)}$ (A,B) or pEGFP-C1/Rab11-FIP2$_{(446–551)}$ (C) were allowed to internalise Alexa 594-Tfn for 45 min at 37 °C. Cells were either fixed at this point (A) or chased for 30 min at 37 °C in the presence of 100-fold excess unlabelled iron saturated Tfn and then fixed (B,C). Arrows indicate transfected cells and arrowheads indicate non-transfected cells. These data are typical of four independent experiments. Scale bar represents 10 μm.

[11,39]. Thus, we were interested to investigate the effects of expression of an amino-terminally truncated mutant of Rab11-FIP3 on Tfn recycling. A construct was made which encodes the carboxy-terminal 513 amino acids of Rab11-FIP3 fused with an amino-terminal EGFP tag (pEGFP-C3/Rab11-FIP3$_{(244–756)}$). This construct encompasses the ARF and Rab11 binding regions of the protein as well as the putative ERM and coiled-coil domains. In HeLa cells, EGFP tagged Rab11-FIP3$_{(244–756)}$ concentrates in the pericentrosomal region of the cell but also localises to peripherally dispersed punctate vesicular structures. In a small proportion of cells, an elaborate tubular Rab11 positive phenotype was observed and in some cells (depending on level of expression) the overexpressed protein localised to the cytoplasm (data not shown).

We sought to investigate the functional effects of overexpression of the amino-terminally truncated mutant of Rab11-FIP3 on the recycling of Tfn to the plasma membrane. HeLa cells expressing pEGFP-C3/Rab11-FIP3$_{(244–756)}$ were allowed to internalise Alexa 594-Tfn for 45 min at 37 °C (uptake). After this loading step, the cells were washed and the ligand was chased for 30 min at 37 °C in the presence of 100-fold excess holotransferrin and the iron-chelator desferroxamine. We found that in cells fixed directly after the loading step, Alexa 594-Tfn had been internalised from the cell surface to the pericentrosomal Rab11-FIP3$_{(244–756)}$ positive compartment as evidenced by the significant colocalisation between Alexa 594-Tfn and the Rab11-FIP3 mutant (Fig. 6A). Overexpression of the mutant does not appear to significantly affect the uptake of the ligand as similar levels of the Alexa 594-Tfn were present in cells overexpressing the Rab11-FIP3 mutant in comparison to non-transfected cells (Fig. 6A). Expression of the amino-terminally truncated mutant of Rab11-FIP3 does not affect the recycling of Tfn, as following the chase; similar levels of Alexa 594-Tfn remain in both transfected and non-transfected cells in the same field of view (Fig. 6B). Interestingly, this differs to what is observed when the carboxy terminus of Rab11-FIP2 is expressed (Fig. 6C and [20]).

These data suggest that overexpression of Rab11-FIP3$_{(244–756)}$ does not significantly perturb Tfn uptake or recycling. This correlates with previously reported data for Arfophilin-2/Rab11-FIP4 [11,39], and is suggestive that Rab11-FIP3 functions as a Rab11 effector in cellular processes other than that involving Tfn recycling.

Discussion

The realisation that Rab11-FIP3 is identical to the previously described ARF interacting protein (Arfophilin) provides tantalising clues that this dual effector protein is likely to play a role in coordinating membrane trafficking and cytokinetic events. However, despite substantial two-hybrid and biochemical evidence supporting a role for Rab11-FIP3 as a Rab11 and ARF effector, little has been documented with respect to either the intracellular distribution of the endogenous protein or its function. In this study, utilising an antibody specific for Rab11-FIP3, we present data that demonstrate the Rab11-FIP3 subcellular localisation in interphase and dividing cells and the dependency of its localisation on various components of the cytoskeleton. We also find that endogenous Rab11-FIP3 resides in a compartment largely distinct to that of the TfnR and demonstrate that it does not participate in Tfn recycling. Based on these findings, and on what has been previously described for Rab11 and ARF6, we suggest that Rab11-FIP3 functions in the delivery of endosomally derived materials to the cleavage furrow during cell division.

Analysis of the subcellular distribution of Rab11-FIP3 demonstrated that Rab11-FIP3 displays a distinct concentrated pericentrosomal-staining pattern in addition to a punctate vesicular pattern dispersed throughout A431 cells. We found that Rab11-FIP3 colocalises with Rab11 in the distinct pericentrosomal compartment. Interestingly, upon investigation of Rab11-FIP3 localisation in HeLa cells, we found that this distinct concentrated pericentrosomal-staining pattern was present only in a small proportion of cells. This observation is likely to be due to a difference in the organisation of endosomal compartments between these two cell types. No colocalisation was observed between Rab11-FIP3 and various markers of the recycling or degradative pathways or the TGN.

Our immunofluorescence experiments were performed using an antibody that specifically recognises endogenous Rab11-FIP3. We show here by immunoblot analysis of A431 and HeLa cell extracts that while its predicted molecular weight is 82.4-kDa, endogenous Rab11-FIP3 migrates at a molecular weight of 130-kDa. We are convinced our antibody is specific for Rab11-FIP3 for several reasons. First, the Rab11-FIP3 immunogen is a peptide unique to Rab11-FIP3 as demonstrated by BLAST analysis. Furthermore, the antibody does not detect other Rab11-FIP purified recombinant proteins. Second, pre-adsorption of the affinity-purified antibody with either purified recombinant GST-Rab11-FIP3$_{(2–246)}$ or the immunising peptide results in complete abolition of Rab11-FIP3 immunoreactivity by both immunoblotting and immunofluorescence. Finally, the antibody detected EGFP tagged Rab11-FIP3 at a molecular weight of 160-kDa. It is unlikely that the larger than expected molecular weight is due to glycosylation or phosphorylation as the recombinant protein (hexahistidine fused) induced in bacteria consistently migrates at a molecular weight in

the region of 140-kDa. The higher than predicted molecular weight that we observe for Rab11-FIP3 may be indicative that Rab11-FIP3 forms SDS resistant dimers as previously reported for the SNAP-25, syntaxin, and synaptobrevin complex [10]. This may well be the case, as the heterotrimeric interaction of SNAP-25, syntaxin, and synaptobrevin involves predicted coiled-coil regions and we have previously shown that Rab11-FIP3 displays extensive predicted coiled-coil motifs and is capable of self-interaction [38].

Upon examination of the localisation of overexpressed EGFP tagged Rab11-FIP3, we found that like the endogenous protein, it localises predominantly to a pericentrosomal compartment where it colocalises extensively with Rab11. Furthermore, we found that similar to what we have previously reported for Rab11-FIP4 [39], overexpression of Rab11-FIP3 causes a condensation of the ERC, as there was a dramatic accumulation of the TfnR and Rab11 into the Rab11-FIP3 positive compartment. This altered morphology that occurs upon overexpression of Rab11-FIP3 suggests that the protein may be involved in determining the organisation of the endosomal recycling compartment.

It is interesting to note that while endogenous RCP displays partial colocalisation with the TfnR [19], we observe little or no co-localisation between Rab11-FIP3 and the TfnR. Furthermore, we have demonstrated through a recycling assay that expression of an amino-terminally truncated mutant of Rab11-FIP3 does not perturb Tfn recycling. This correlates with what has been previously shown for Arfophilin-2/Rab11-FIP4 [11,39] and contrasts with what has been previously described for class I Rab11-FIPs (RCP and Rab11-FIP2) [19,20]. Overall, these findings demonstrate that functional differences exist between Rab11-FIP3 and the class I Rab11-FIPs. Taken together, these data suggest that class II Rab11-FIPs (Rab11-FIP3 and Rab11-FIP4) are likely to serve as effectors in Rab11 mediated cellular processes not involving transferrin recycling.

The work of Shin and co-workers [31,32], which proposes that Rab11-FIP3 is a class II and class III ARF effector, led us to investigate its localisation with respect to overexpressed ARF4, -5, and -6. While it has been demonstrated through GST pulldown assays and yeast two-hybrid screening that Rab11-FIP3 interacts with the overexpressed GTP-locked mutants of class II and class III ARFs [31,32], we did not detect any colocalisation between Rab11-FIP3 and ARF4 or -5 by immunofluorescence. We did observe minor colocalisation between Rab11-FIP3 and ARF6 in cells undergoing cytokinesis. It is also interesting to note that we observed no perturbation of the localisation of endogenous Rab11-FIP3 upon overexpression of ARF mutants. Furthermore, while Hickson and co-workers [11] found that BFA treatment affected the localisation of endogenous Arfophilin-2/Rab11-FIP4 we found no such effect for Rab11-FIP3. Our results show that following treatment with BFA, both the TfnR and TGN46 displayed a distinct tubulated staining pattern, but the Rab11-FIP3 staining was not affected and did not enter these tubules. It is possible that the interactions between Rab11-FIP3 and ARF GTPases are only relevant at certain points of the cell cycle (see below), or that Rab11-FIP3 localisation is unaffected by BFA treatment because some ARF GEFs are insensitive to BFA as has been documented for ARF6 GEFs [12]. Unquestionably, further study is required to fully understand the interactions between Rab11-FIP3 and ARF proteins.

Our observations suggest that Rab11-FIP3 localisation is dependent on the integrity of two components of the cytoskeleton. We found that disruption of the microtubule network by nocodazole causes the Rab11-FIP3 positive ERC to fragment. This was not surprising as it has been previously documented that the localisation of other Rab11-FIP family members is affected upon breakdown of the microtubule cytoskeleton [11,20]. It is conceivable, since Rab11 and Rab11-FIP3 colocalise with microtubules within the intercellular bridge during cytokinesis, that either Rab11 or Rab11-FIP3 might function in motor protein recruitment or regulation. Such recruitment or regulation may deliver cargo from the ERC to the cleavage furrow during the latter stages of cell division. This model is compatible with data on nuclear-fallout (Nuf), the *Drosophila melanogaster* orthologue of Rab11-FIP3/Rab11-FIP4 which is required for cellularisation in *Drosophila* [27,28] and displays a similar localisation to Rab11-FIP3 when overexpressed in mammalian cells [11]. Furthermore, Nuf has been shown to interact with Rab11 [26] and is believed to load vesicles onto microtubules for transport to furrows in *Drosophila* [28,42].

Our observation that a cytochalasin D sensitive population of Rab11-FIP3 exists suggests a Rab11-FIP3 association with actin. This observation in conjunction with previously published data that Nuf inhibits both membrane recruitment and actin remodelling at the early stages of furrow formation [26,28,42] further supports a role for Rab11-FIP3 in actin based motility/dynamics. This interaction could be mediated indirectly via Rab11 binding of MyosinVb [16] or could directly involve the Rab11-FIP3 ERM domain.

We have demonstrated that both Rab11 and Rab11-FIP3 distribute to the cleavage furrow during cytokinesis. Given that Rab11-FIP3 is both a Rab11 and ARF6 effector protein, and taking into account what has been previously shown for both Rab11 and ARF6 during cytokinesis, it is reasonable to suggest that Rab11-FIP3 may well provide a link between these two GTPases during this process. Elucidating this link is currently a focus of ongoing research in our laboratory.

Acknowledgments

The authors are grateful to T. Nagase (Kazusa DNA Research Institute, Japan) for the cDNA encoding Rab11-FIP3 (KIAA0665); C. D'Souza-Schorey (University of Notre Dame, Indiana, USA) for the ARF6 cDNA; A. Hendrick (University of Cambridge, UK) for the ARF4 and -5 constructs; R. Pepperkok (EMBL Heidelberg, Germany) for the GFP[2] plasmids; J. Gruenberg (University of Geneva, Switzerland) for the anti-LBPA antibody; and A. Lindsay for the anti-Rab11 and anti-RCP antibodies. The authors also wish to thank N. Marie, S. Hanscom, and A. Lindsay for helpful discussions during the preparation of the manuscript. The project was supported by the Irish Research Council for Science, Engineering and Technology (IRCSET) (Grant # RS/2002/202-6) to C.H., the European Union (Marie Curie Development Host Fellowship, Grant # HPMD-CT-2000-00024), and Science Foundation Ireland (SFI), (Investigator Grant # 02/IN.1/B070) to M.M.C.

References

[1] G. Apodaca, L.A. Katz, K.E. Mostov, Receptor-mediated transcytosis of IgA in MDCK cells is via apical recycling endosomes, J. Cell Biol. 125 (1994) 67–86.

[2] W.E. Balch, R.A. Kahn, R. Schwaninger, ADP-ribosylation factor is required for vesicular trafficking between the endoplasmic reticulum and the *cis*-Golgi compartment, J. Biol. Chem. 267 (1992) 13053–13061.

[3] P. Chavrier, B. Goud, The role of ARF and Rab GTPases in membrane transport, Curr. Opin. Cell Biol. 11 (1999) 466–475.

[4] H. Cheng, R. Sugiura, W. Wu, M. Fujita, Y. Lu, S.O. Sio, R. Kawai, K. Takegawa, H. Shuntoh, T. Kuno, Role of the Rab GTP-binding protein Ypt3 in the fission yeast exocytic pathway and its connection to calcineurin function, Mol. Biol. Cell 13 (2002) 2963–2976.

[5] J.G. Donaldson, Multiple roles for Arf6: sorting, structuring, and signaling at the plasma membrane, J. Biol. Chem. 278 (2003) 41573–41576.

[6] F.P. Finger, J.G. White, Fusion and fission: membrane trafficking in animal cytokinesis, Cell 108 (2002) 727–730.

[7] E.C. Gaynor, C.Y. Chen, S.D. Emr, T.R. Graham, ARF is required for maintenance of yeast Golgi and endosome structure and function, Mol. Biol. Cell 9 (1998) 653–670.

[8] F. Gu, J. Gruenberg, ARF1 regulates pH-dependent COP functions in the early endocytic pathway, J. Biol. Chem. 275 (2000) 8154–8160.

[9] C.M. Hales, R. Griner, K.C. Hobdy-Henderson, M.C. Dorn, D. Hardy, R. Kumar, J. Navarre, E.K. Chan, L.A. Lapierre, J.R. Goldenring, Identification and characterization of a family of Rab11-interacting proteins, J. Biol. Chem. 276 (2001) 39067–39075.

[10] T. Hayashi, H. McMahon, S. Yamasaki, T. Binz, Y. Hata, T.C. Sudhof, H. Niemann, Synaptic vesicle membrane fusion complex: action of clostridial neurotoxins on assembly, Embo J. 13 (1994) 5051–5061.

[11] G.R. Hickson, J. Matheson, B. Riggs, V.H. Maier, A.B. Fielding, R. Prekeris, W. Sullivan, F.A. Barr, G.W. Gould, Arfophilins are dual Arf/Rab 11 binding proteins that regulate recycling endosome distribution and are related to *Drosophila* nuclear fallout, Mol. Biol. Cell 14 (2003) 2908–2920.

[12] C.L. Jackson, J.E. Casanova, Turning on ARF: the Sec7 family of guanine-nucleotide-exchange factors, Trends Cell Biol. 10 (2000) 60–67.

[13] R.A. Kahn, F.G. Kern, J. Clark, E.P. Gelmann, C. Rulka, Human ADP-ribosylation factors. A functionally conserved family of GTP-binding proteins, J. Biol. Chem. 266 (1991) 2606–2614.

[14] R.D. Klausner, J.G. Donaldson, J. Lippincott-Schwartz, Brefeldin A: insights into the control of membrane traffic and organelle structure, J. Cell Biol. 116 (1992) 1071–1080.

[15] T. Kobayashi, E. Stang, K.S. Fang, P. de Moerloose, R.G. Parton, J. Gruenberg, A lipid associated with the antiphospholipid syndrome regulates endosome structure and function, Nature 392 (1998) 193–197.

[16] L.A. Lapierre, R. Kumar, C.M. Hales, J. Navarre, S.G. Bhartur, J.O. Burnette, D.W. Provance Jr., J.A. Mercer, M. Bahler, J.R. Goldenring, Myosin vb is associated with plasma membrane recycling systems, Mol. Biol. Cell 12 (2001) 1843–1857.

[17] J.O. Liang, S. Kornfeld, Comparative activity of ADP-ribosylation factor family members in the early steps of coated vesicle formation on rat liver Golgi membranes, J. Biol. Chem. 272 (1997) 4141–4148.

[18] S.X. Lin, B. Grant, D. Hirsh, F.R. Maxfield, Rme-1 regulates the distribution and function of the endocytic recycling compartment in mammalian cells, Nat. Cell Biol. 3 (2001) 567–572.

[19] A.J. Lindsay, A.G. Hendrick, G. Cantalupo, F. Senic-Matuglia, B. Goud, C. Bucci, M.W. McCaffrey, Rab coupling protein (RCP), a novel Rab4 and Rab11 effector protein, J. Biol. Chem. 277 (2002) 12190–12199.

[20] A.J. Lindsay, M.W. McCaffrey, Rab11-FIP2 functions in transferrin recycling and associates with endosomal membranes via its COOH-terminal domain, J. Biol. Chem. 277 (2002) 27193–27199.

[21] J. Moss, M. Vaughan, Structure and function of ARF proteins: activators of cholera toxin and critical components of intracellular vesicular transport processes, J. Biol. Chem. 270 (1995) 12327–12330.

[22] F.T. Mu, J.M. Callaghan, O. Steele-Mortimer, H. Stenmark, R.G. Parton, P.L. Campbell, J. McCluskey, J.P. Yeo, E.P. Tock, B.H. Toh, EEA1, an early endosome-associated protein. EEA1 is a conserved alpha-helical peripheral membrane protein flanked by cysteine fingers and contains a calmodulin-binding IQ motif, J. Biol. Chem. 270 (1995) 13503–13511.

[23] T. Nagase, K. Ishikawa, R. Kikuno, M. Hirosawa, N. Nomura, O. Ohara, Prediction of the coding sequences of unidentified human genes. XV. The complete sequences of 100 new cDNA clones from brain which code for large proteins in vitro, DNA Res. 6 (1999) 337–345.

[24] S. Ponnambalam, M. Girotti, M.L. Yaspo, C.E. Owen, A.C. Perry, T. Suganuma, T. Nilsson, M. Fried, G. Banting, G. Warren, Primate homologues of rat TGN38: primary structure, expression and functional implications, J. Cell Sci. 109 (Pt. 3) (1996) 675–685.

[25] R. Prekeris, J.M. Davies, R.H. Scheller, Identification of a novel Rab11/25 binding domain present in Eferin and Rip proteins, J. Biol. Chem. 276 (2001) 38966–38970.

[26] B. Riggs, W. Rothwell, S. Mische, G.R. Hickson, J. Matheson, T.S. Hays, G.W. Gould, W. Sullivan, Actin cytoskeleton remodeling during early *Drosophila* furrow formation requires recycling endosomal components Nuclear-fallout and Rab11, J. Cell Biol. 163 (2003) 143–154.

[27] W.F. Rothwell, P. Fogarty, C.M. Field, W. Sullivan, Nuclear-fallout, a *Drosophila* protein that cycles from the cytoplasm to the centrosomes, regulates cortical microfilament organization, Development 125 (1998) 1295–1303.

[28] W.F. Rothwell, C.X. Zhang, C. Zelano, T.S. Hsieh, W. Sullivan, The *Drosophila* centrosomal protein Nuf is required for recruiting Dah, a membrane associated protein, to furrows in the early embryo, J. Cell Sci. 112 (Pt. 17) (1999) 2885–2893.

[29] S.L. Schmid, P.R. Cullis, Membrane sorting. Endosome marker is fat not fiction, Nature 392 (1998) 135–136.

[30] J.K. Schweitzer, C. D'Souza-Schorey, Localization and activation of the ARF6 GTPase during cleavage furrow ingression and cytokinesis, J. Biol. Chem. 277 (2002) 27210–27216.
[31] O.H. Shin, A.D. Couvillon, J.H. Exton, Arfophilin is a common target of both class II and class III ADP-ribosylation factors, Biochemistry 40 (2001) 10846–10852.
[32] O.H. Shin, A.H. Ross, I. Mihai, J.H. Exton, Identification of arfophilin, a target protein for GTP-bound class II ADP-ribosylation factors, J. Biol. Chem. 274 (1999) 36609–36615.
[33] A. Simonsen, R. Lippe, S. Christoforidis, J.M. Gaullier, A. Brech, J. Callaghan, B.H. Toh, C. Murphy, M. Zerial, H. Stenmark, EEA1 links PI(3)K function to Rab5 regulation of endosome fusion, Nature 394 (1998) 494–498.
[34] A.R. Skop, D. Bergmann, W.A. Mohler, J.G. White, Completion of cytokinesis in *C. elegans* requires a brefeldin A-sensitive membrane accumulation at the cleavage furrow apex, Curr. Biol. 11 (2001) 735–746.
[35] O. Ullrich, S. Reinsch, S. Urbe, M. Zerial, R.G. Parton, Rab11 regulates recycling through the pericentriolar recycling endosome, J. Cell Biol. 135 (1996) 913–924.
[36] P. van der Sluijs, M. Hull, P. Webster, P. Male, B. Goud, I. Mellman, The small GTP-binding protein rab4 controls an early sorting event on the endocytic pathway, Cell 70 (1992) 729–740.
[37] P. Van Der Sluijs, M. Hull, A. Zahraoui, A. Tavitian, B. Goud, I. Mellman, The small GTP-binding protein rab4 is associated with early endosomes, Proc. Natl. Acad. Sci. USA 88 (1991) 6313–6317.
[38] D.M. Wallace, A.J. Lindsay, A.G. Hendrick, M.W. McCaffrey, The novel Rab11-FIP/Rip/RCP family of proteins displays extensive homo- and hetero-interacting abilities, Biochem. Biophys. Res. Commun. 292 (2002) 909–915.
[39] D.M. Wallace, A.J. Lindsay, A.G. Hendrick, M.W. McCaffrey, Rab11-FIP4 interacts with Rab11 in a GTP-dependent manner and its overexpression condenses the Rab11 positive compartment in HeLa cells, Biochem. Biophys. Res. Commun. 299 (2002) 770–779.
[40] M. Wilcke, L. Johannes, T. Galli, V. Mayau, B. Goud, J. Salamero, Rab11 regulates the compartmentalization of early endosomes required for efficient transport from early endosomes to the *trans*-golgi network, J. Cell Biol. 151 (2000) 1207–1220.
[41] M. Zerial, H. McBride, Rab proteins as membrane organizers, Nat. Rev. Mol. Cell Biol. 2 (2001) 107–117.
[42] C.X. Zhang, W.F. Rothwell, W. Sullivan, T.S. Hsieh, Discontinuous actin hexagon, a protein essential for cortical furrow formation in *Drosophila*, is membrane associated and hyperphosphorylated, Mol. Biol. Cell 11 (2000) 1011–1022.